pagepress

Journal of Agricultural Engineering

Journal of Agricultural Engineering 2026; LVII:1936
doi:10.4081/jae.2026.1936

Development of a "PCM-in-container" energy storage model component for a possible building energy evaluation in TRNSYS 18

Qazeem Opeyemi Ogunlowo,[1,2] Timothy Denen Akpenpuun,[3] Wook Ho Na,[1] Misbaudeen Aderemi Adesanya,[4] Anis Rabiu,[1] Adedayo Afeez Azeez,[2] Ayoade Oladele Atere,[2] Hyun-Woo Lee,[5] Sangik Lee[5]

[1]Institute of Agricultural Science and Technology, Kyungpook National University, Daegu, Korea; [2]Department of Agricultural and Bioenvironmental Engineering, Federal College of Agriculture Ibadan, Nigeria; [3]Department of Agricultural and Biosystems Engineering, University of Ilorin, Nigeria: [4]Future Urban and Energy Lab for Sustainability (FUEL-S), Faculty of Sustainable Design Engineering (FSDE), University of Prince Edward Island, Charlottetown, Canada; [5]Department of Agricultural Civil Engineering, College of Agricultural and Life Sciences, Kyungpook National University, Daegu, Korea

Abstract

Phase change materials (PCMs) offer a promising pathway toward net-zero energy buildings by enhancing thermal energy efficiency. By absorbing and storing heat during the day and releasing it at night, PCMs can reduce reliance on active heating and cooling systems. While PCMs have been widely studied both experimentally and numerically, limited research exists on configurations where PCM containers are in direct contact with surrounding air. This study developed a novel "PCM-in-container" component in TRNSYS 18 to simulate energy gains from such direct interactions. The component was integrated with greenhouse and weather modules in TRNSYS and validated experimentally using three model greenhouses containing air, water, and Vaseline as PCM substances. Model performance was assessed using R-squared (R^2), correlation coefficient (CC), root mean square error (RMSE) and mean absolute error (MAE). For water-based PCM, values of $R^2 = 0.97$, CC = 0.99, RMSE = 2.01°C, and MAE = 1.33°C were obtained, demonstrating strong model accuracy. The results showed that PCM-filled containers (e.g., structural or railing pipes) could increase nighttime greenhouse temperatures by up to 7°C. The developed component enables energy gain simulations and nighttime heating predictions, offering a valuable tool for greenhouse energy demand evaluation. Although the current model does not account for hysteresis, future work may incorporate this through modifications in the TRNSYS Fortran environment.

Key words: PCM component; TRNSYS 18; air temperature; energy storage; greenhouse.

Correspondence: Sangik Lee, Department of Agricultural Civil Engineering, College of Agriculture and Life Sciences, Kyungpook National University, 80 Daehak-ro, Buk-gu, Daegu, Republic of Korea. E-mail: sangik@knu.ac.kr

Introduction

According to Kutty *et al.* (2023), building heating and cooling requires approximately 93% of the building's total energy demand. Thus, net-zero energy buildings (NZEB) can be achieved if the heating and cooling needs are drastically reduced. One way to achieve NZEB is by using phase change materials (PCMs). According to Jayalath *et al.* (2016), PCMs offer a convenient method for improving energy efficiency in buildings by delaying heat transfer during the day, storing energy, and releasing the obtained energy at night or during cooler periods. In addition, building materials incorporating PCMs could store significant thermal energy within the building envelope using less structural mass than sensible heat storage (Boussaba and Lefebvre, 2021). The energy gain may be sensible storage or both sensible and latent storage, depending on whether the phase change temperature is reached. To assess the thermal performance of buildings with PCMs installed, experimental (Zhao *et al.*, 2023) and numerical (Najjar and Hasan, 2008; Jayalath *et al.* 2016; Naghibi and Ting, 2019) methods have been employed. Using building energy simulation (BES) software tools, thermal performance investigations with various PCMs and placement methods within a building envelope have been conducted (Jayalath *et al.*, 2016).

Cabeza *et al*. (2011) and Nishad and Krupa (2022) separately reviewed materials used as PCM in building and greenhouses, respectively and concluded that the solid-liquid PCMs can either be organic or inorganic, with both being eutectics (single temperature) or mixtures (temperature intervals). The organics are further categorized as paraffin or fatty acids, while the inorganics are mainly hydrated salts. In greenhouse application, the review by Mu *et al.* (2022) stated that Paraffin wax, fatty acids and methyl eicosanoate are the most organic PCMs used; Cobalt II chloride as the inorganic; and mixture of 60% decanoic acid 40% oleic acid as the eutectic PCMs used. Among the materials mentioned by Cabeza *et al*. (2011) and Mu *et al.* (2022) is water with 0°C melting point which makes it a potential PCM for systems in temperate regions.

In an attempt to determine the most accurate PCM-BES tools, Mazzeo *et al*. (2020) investigated IDA ICE, EnergyPlus, and TRN-

SYS (Transient Systems Simulation program, developed by the University of Wisconsin) as the most popular BES tools. Cornaro *et al.* (2017) created a PCM wall in the IDA ICE tool to simulate Rubitherm S21E behavior and evaluate its capability to reduce heating and cooling loads inside an office building for various climates in Italy. In the case of Jayalath *et al.* (2016) and Panayiotou *et al.* (2016), a PCM wall called "Type 1270" was developed and validated in TRNSYS 16, and was used to evaluate the thermal performance of a single-story residential building in Australia. Additional model test cells with PCM in the walls, referred to as Types 260, 241, and 204, linked with Type 56 (Multizone Building), were developed by Schranzhofer *et al.* (2006), Virgone *et al.* (2010), and Poulad *et al.* (2011), respectively.

PCMs applied in greenhouses have been studied by different researchers and are reviewed by Mu *et al.* (2022) and Nishad and Krupa (2022). Nishad and Krupa (2022) listed the applications of PCMs to control greenhouse microclimates as active and passive systems. While the active systems included i) PCMs integrated with heaters and heat pumps and ii) PCMs integrated with solar thermal collectors, the passive systems included i) PCM wallboards, and ii) PCM storage inside containers. Plastic greenhouses without north walls are primarily used in continental temperate regions, such as Korea, where the summer season is hot and the winter season is cold. Such environments are suitable for placing PCM-filled containers inside the greenhouses. For this application, most research has been experimental. For example, Rieradevall *et al.* (2017) studied the use of Rubitherm12, 15, and 18HC, for root zone heating in Mediterranean greenhouses by placing the substrates in the greenhouses, and the PCM's melting point was successfully determined for the studied crop. Recently, Zhao *et al.* (2023) experimentally evaluated the effect of water and organic paraffin on the indoor temperature of a greenhouse. Their results showed that it was possible to increase the night temperature of the greenhouse by 10°C. The authors, however, recommended that the relationship between the PCM temperature effect and crop yield. These results could be achieved faster and at less expense if a numerical method was adopted.

Unlike office and residential buildings, greenhouses are numerically characterized by thin external walls with extensive glazing. The structure will depend on the type of greenhouse. For example, a double-layer single-span greenhouse as described by Akpenpuun *et al*. (2021a, 2021b), Ogunlowo *et al.* (2021) and Zakir *et al*. (2022), apart from the external walls made of a steel structure, consists of a second layer held by another steel structure which is in contact with the internal air. The aforementioned "Types" (260, 241, and 204) in TRNSYS 16 were designed to interact with Type 56 when a PCM layer is integrated into walls in contact with both boundary surfaces within a thermal zone. Consequently, the "Types" cannot be used when the PCM layer directly interacts with the thermal air node and the walls connected to the outdoor environment (Mazzeo *et al.*, 2020). Additionally, TRNSYS has released two new versions, with TRNSYS 18 being the latest, which has been used by researchers to simulate the internal temperature and heating demand of a glass greenhouse (Adesanya *et al.*, 2022) study the effect of the software envelope characteristics on the accuracy of building models developed in TRNSYS (Ogunlowo *et al.*, 2022), and determine the overall heat transfer coefficient of greenhouse energy saving screens (Rabiu *et al*.. 2022), among others. This new version of TRNSYS requires a PCM component that works in direct contact with internal air. Hence, the following questions arose. i) Can such a PCM component be created in TRNSYS 18? ii) If yes and if it can be validated, can it then be used to evaluate the greenhouse's thermal change?

This research aimed to develop a PCM component with direct air interaction in TRNSYS 18 and then evaluate its performance within the greenhouse's thermal environment. If successful, this component can be linked to greenhouse buildings (Type 56) and other component types to evaluate the system's energy demand. It will also help in the numerical evaluation of PCM applications for root zone heating. The novel component will make it possible to study the effect of PCMs stored in energy storage devices in contact with direct air within a greenhouse and other structures using TRNSYS. A novel feat which before now, only allowed for PCM in walls.

Materials and Methods

Figure 1 shows a typical interior of a double-layer single-span greenhouse, which is common in South Korea. Figure 1a displays the first layer and crop bench frames made of steel pipes. Figure 1b shows the boiler system's heat exchanger pipe. The boiler and the pipes are typically filled with water for nighttime or cold day heating. This study proposes that the bench frame (BF) and heat exchanger (HE) pipes are filled with PCMs, and the amount of heat energy contributed by the boiler will then be evaluated when raising the greenhouse air temperature. The results will indicate whether the volume of greenhouse gas emissions has been reduced. Hence, in this section, the PCM component was developed and validated using a method similar to Jayalath *et al*. (2016) and Cornaro *et al.* (2017). The developed PCM component was linked to a greenhouse and other components in the TRNSYS Simulation Studio, as shown in Figure 2. The regime definition and setting in TRNBuild - an interface for creating and editing all of the non-geometry information required by the TRNSYS Building Model. TRNBuild allows the user extensive flexibility in editing wall and layer material properties, creating ventilation and infiltration profiles, adding gains, defining radiant ceilings and floors, and positioning occupants for comfort calculations (TRANSSOLAR Energietechnik 2017) - and properties of glazing materials have

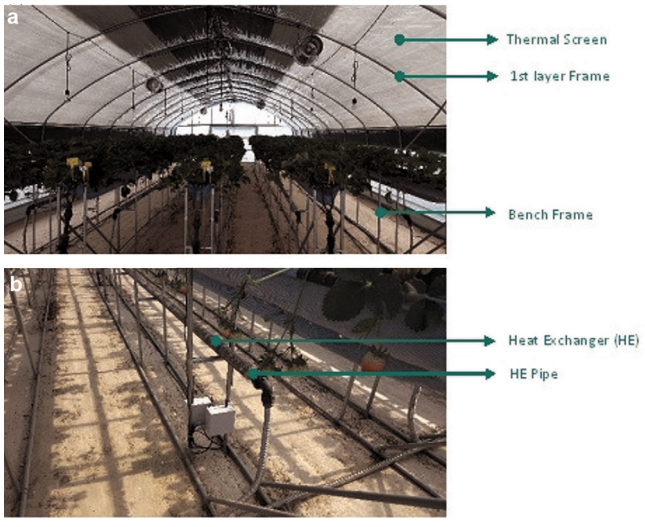

Figure 1. Typical double-layer single-span greenhouse in Korea: (**a**) indoor support structures; (**b**) heating system.

been well explained by previous studies by Ogunlowo *et al.* (2022, 2023), thereby, this study only focuses on the PCM component development. After validation, the greenhouse thermal variation was evaluated.

PCM component development

Figure 3 shows the flowchart for developing the PCM component (Type 207) in TRNSYS 18. A proforma was first created in TRNSYS Simulation Studio, where the "Type" name was given, and the parameters, inputs, and outputs were defined (Table 1). The proforma was, thereafter, exported to a Fortran environment in Type Studio, where the model equation was edited, and the boundary conditions were set. It was then compiled and saved in the Simulation Studio, ready to be coupled with other components.

The energy equation was temperature-based, as shown in Eqs. 1-3. The sensitive heat flow was represented by Eq. 1, while Eq. 2 represents the latent heat flow. The phase equilibrium state can be represented by the Eq 3. At this point, the solid, melting and liquid phases co-existed and are duly represented in the model:

$$\dot{q}(\text{kJ/hr}) = mc\Delta T = \rho V c \Delta T \qquad (Sensible\ heat) \qquad \text{(Eq. 1)}$$

$$\dot{q}(\text{kJ/hr}) = mL = \rho V L \qquad (Latent\ heat/phase\ change) \qquad \text{(Eq. 2)}$$

$$\dot{q}(\text{kJ/hr}) = [\rho_s V_s c_s (T_f - T_i) + \rho_p V_p L + \rho_l V_l c_l (T_f - T_i)] + \rho_c V_c c_c (T_f - T_i) \qquad \text{(Eq. 3)}$$

where is the energy rate (gain or loss) (kJ·hr^{-1}), m is the mass of the PCM (kg), c is the specific heat capacity of PCM (kJ·kg^{-1}K^{-1}), DT is the change in temperature (°C), r is the density of PCM (kg·m^{-3}), V is the volume of PCM (m^3), and L is the latent heat of PCM (kJ·kg^{-1}). The subscripts *s, p*, and *l* represent the properties of the PCM phases at solid, phase change, and liquid, respectively, and *c* represent the properties of the container. Finally, T_f and T_i represents the material temperature at the final timestep (i.e. $i+1$) and the initial timestep (i).

In Eqs. 4-6, T_i represents the material temperature at the current timestep (i), while T_f represents the updated temperature at the next timestep ($i+1$). The governing equation applied at each timestep depends on the material's thermodynamic state relative to the melting temperature (T_m).

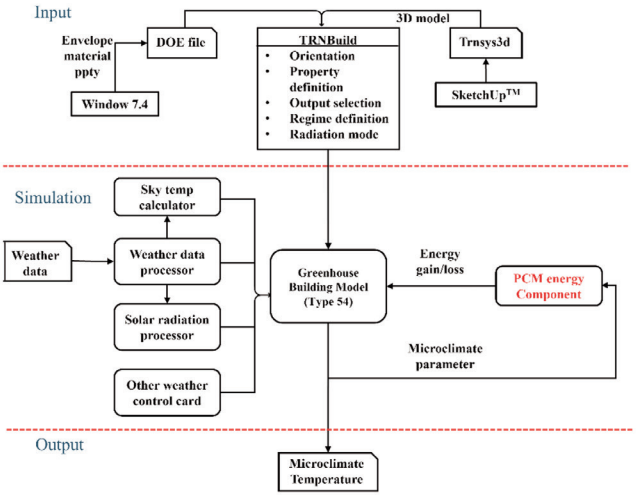

Figure 2. Flowchart of the model simulation in TRNSYS 18.

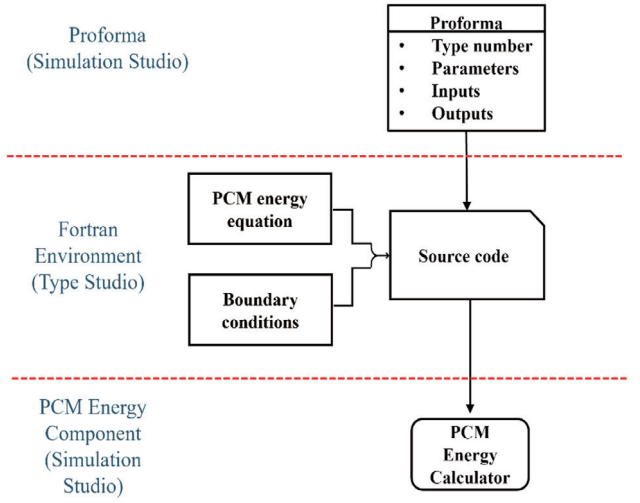

Figure 3. Flowchart of PCM component (Type 207) development.

Table 1. Phase change material (PCM) component parameter, input, and output definition in TRNSYS simulation studio.

Variable name	Role	Unit
Specific heat capacity of the PCM	Parameter	kJ·kg^{-1}K^{-1}
Density of the PCM	Parameter	kg·m^{-3}
Thermal conductivity of the PCM	Parameter	kJ.(hr.mK)$^{-1}$
Air temperature	Input	°C
Volume of the PCM	Input	m^3
Latent heat of the PCM	Parameter	kJ·kg^{-1}
Melting Point of the PCM	Parameter	°C
Specific heat capacity of the container	Parameter	kJ·kg^{-1}K^{-1}
Density of the container	Parameter	kg·m^{-3}
Volume of the container	Input	m^3
Energy storage rate	Output	kJ·hr^{-1}

At each timestep, the procedure is:

1. Determine the initial state using T_i:

If $T_i < T_m$, the material is in the solid phase → Eq. (4) is applied (sensible heat in solid state).

If $T_i = T_m$the material is undergoing phase change → Eq. (5) is applied (latent heat process, temperature remains constant).

If $T_i > T_m$, the material is in the liquid phase → Eq. (6) is applied (sensible heat in liquid state).

2. Compute the updated temperature T_f: the selected energy balance equation is solved over the timestep Dt to obtain T_f.

3. Advance the timestep: the computed T_f becomes the new T_i for the next timestep $(i+1)$.

Thus, the decision logic controlling Eqs. 4-6 is a phase-dependent, forward time-marching scheme in which the governing heat storage term switches between solid sensible heat, latent heat, and liquid sensible heat formulations based on the material temperature relative to T_m. To calculate the energy flow rate at different phases, the boundary conditions are set as shown in Eqs. 4 to 6. At a solid state when the PCM initial temperature is less than its melting point, the equation deployed was in Eq. 4. In contrast, Eq. 6 is deployed when it is at its liquid state, *i.e.* when the initial temperature is higher than its melting point. Finally, the Eq. 5 is deployed when the PCM is at its melting phase. The initial, melting and final temperature of the PCM are set at the same value.

$$\dot{q}(\mathrm{kJ\cdot hr^{-1}}) = \rho_s V_s c_s (T_f - T_i) + \rho_c V_c c_c (T_f - T_i) \quad (T_i < T_m) \quad \text{(Eq. 4)}$$

$$\dot{q}(\mathrm{kJ\cdot hr^{-1}}) = \rho_p V_p L + \rho_c V_c c_c (T_f - T_i) \quad (T_f = T_i = T_m) \quad \text{(Eq. 5)}$$

$$\dot{q}(\mathrm{kJ\cdot hr^{-1}}) = \rho_l V_l c_l (T_f - T_i) + \rho_c V_c c_c (T_f - T_i) \quad (T_i > T_m) \quad \text{(Eq. 6)}$$

As shown in Figure 2, the simulation input for the PCM energy components is the building (greenhouse) microclimate air temperature. To ensure the component is applicable to other structures, the volume of the structure and type of container are also set as input, as presented in Table 1.

Reference greenhouse

The reference greenhouse (RGH) is a double-layer single-span greenhouse at Kyungpook National University's Smart Farm Center in Daegu, South Korea. The first layer is an 18 x 6.5 m floor area, enclosed in a 24 x 7 m second layer. During the evaluation period (20th to 22nd of February 2022), both layers are enveloped by a polyolefin (PO) screen at night (6 pm-9 am), with an additional thermal screen (TS) layer on top of the first layer. During the day (9 am-6 pm), the envelopes on the first layer are rolled up, making the greenhouse single-layered during this period. Figure 4 shows a skeletal view of the RGH. The first layer frame (FLF), bench frame (BF), and heat exchanger (HE) pipes are all potential PCM containers and are considered in this study. The FLF carries the weight of the layer envelopes (PO and TS). The BF carries the weight of the crop and its substrate. The HE pipes link together and connect to the boiler tank. These pipes are filled with water and used to dissipate supplemental heat supplied by the boiler during cold nights and days.

In theory, as a member of PCMs, the stored water in the boiler system should gain energy when the greenhouse air temperature is and rises above its melting point of 0°C during the day *via* solar gain in the greenhouse and release that energy at night when the greenhouse temperature plummets below 0°C during the winter season. The contribution of this system to the nighttime greenhouse temperature will be assessed through the development of the PCM component.

Model greenhouse

Three scaled-down model greenhouses (MGs) were constructed to represent the enclosed first layer of the RGH. Seo (2018) claims that the models' arguments include the ability to control flow and ambient conditions and the fact that they are modest in comparison to their actual size, which results in inexpensive implementation costs. The process is based on the law of similitude, which, according to Chanson (2009) and Eydani Asl *et al.* (2017),

Table 2. Thermophysical properties and price of phase change materials.

Property	Vaseline	Water
Specific heat capacity (kJ·kg^{-1}K^{-1})	2.13[#]	4.186^
Density (kg·m^{-3})	820§	998^
Thermal conductivity (kJ·(hr. mK)$^{-1}$)	0.96[#]	2.16^
Heat of fusion (kJ·kg^{-1})	95.38[§]	333^
Melting point (°C)	36.56[§]	0^
Price (Won)	7.973/mL[&]	0.7478/L°

[#]Engineering ToolBox (https://www.engineeringtoolbox.com/specific-heat-fluids-d_151.html); [§]Boussaba and Lefebvre (2021); ^Cabeza *et al.* (2011); °Yoo (2024); [&]Care to Beauty (https://www.caretobeauty.com/kr/vaseline-original-protecting-jelly/)

Table 3. Characteristics of the model and actual-size greenhouse.

Characteristics	Model size	Actual size
Volume of filling (m^3)	0.0000204	0.1634
Volume of pipe (m^3)	0.0000102	0.0817
Density of pipe (kg·m^{-3})	2700	2700
Specific heat capacity of the aluminum pipe (kJ·kg–1K–1)	0.89	0.89
Greenhouse area (m^2)	0.288	117
Greenhouse volume (m^3)	0.041	327.04
Ratio of filling-to-greenhouse volume	0.000499	0.000499

it is achieved when testing conditions are created such that the test results are applicable to the real design. Chanson (2009) and Eydani Asl *et al.* (2017) further stated that three conditions are required for a model to have similitude with an actual-sized system, which are:

- Geometric similarity – the model is the same shape as the application, usually scaled.
- Kinematic similarity – fluid flow of both the model and real application must undergo similar rates of change in motions i.e. fluid streamlines are similar.
- Dynamic similarity – ratios of all forces acting on corresponding fluid particles and boundary surfaces in the two systems are constant.

The MG-to-actual size ratio was scaled to 1:20 to fulfil the first condition. Having met the first condition, a similar shape was maintained to ensure the second condition was also met, which, according to Seo (2018) flows with geometric streamlines are kinetically similar. Finally, the third condition was met by ensuring the boundary conditions, such as shape (Eydani Asl *et al.,* 2017), and net force on the model and actual size greenhouse is zero in both cases are similar. To model the PCM-filled FLF and BF pipes, the pipe volume was scaled down by the same ratio and represented by a framing pipe (FP). Each FP was separately filled with air (base condition), water, and vaseline (PCM). The PCMs were selected based on cost and availability (Table 2).

Tables 2 and 3 show the properties of the selected materials and the greenhouse characteristics, respectively. Figure 5 shows the dimensions of the MGs in various views. Hobo Onset U23-002 sensors, with a sensitivity of ±0.21°C (from 0°C to 50°C) were installed in the MGs to record the microclimate temperature every 10 min. Figure 6 shows the arrangement of the MGs with and without the thermal screen. On day one (February 19th) of the experiment, the three MGs were without the PCM container; this was to observe the microclimate conditions within the MGs before PCM installation. On day two, the TS was not installed. On day three, the TS was installed at night. To visualize the temperature gradient during the experimental process, FLIR thermal imaging camera (model: FLIR-T62101) was acquired. The camera a high quality device equipped with a host of rich features, including superior thermal imaging with resolution of 76,800 pixels for solid accuracy; a compass which adds camera pointing direction to every image for location documentation; accurate temperature measurement within ±2°C; high temperature range up to -20°C to 650°C; spectral range of 7.5 to 13 µm, and frame rate of 60 Hz among others.

Model validation

To validate the model, experimentation was conducted using the three MGs. The experimental setup was located on the roof of the Department of Agricultural Civil Engineering at Kyungpook National University, in Daegu, South Korea. Every 10 minutes, the following measurements were recorded: temperature of the MG's microclimate, ambient temperature, relative humidity, wind speed, wind direction, horizontal solar radiation, and pressure.

In the simulation, the PCM component was linked to the building component, and the ambient recorded data collected during the winter season (February 19-21, 2023) were used, as shown in Figure 2. Unlike in the experiment where the TS was not deployed on day two, the TS was simulated for two days; this was to check the effect of the TS on the nighttime temperature. The output of the simulation–air temperature–was compared with the microclimate temperature from the experimental MGs using the following metrics: R-squared (R^2) Eq. 7 (Ogunlowo *et al.*, 2022), root mean square error (RMSE) Eq. 8 (Jayalath *et al.*, 2016; Cornaro *et al.*, 2017), mean absolute error (MAE) Eq. 9, and correlation coefficient (CC) Eq. 10 (Jayalath *et al.*, 2016). While R^2 indicates how well the experimental temperature matches the simulated temperature, the RMSE and MAE indicate the magnitude of the error between the two (Benjamin, 2020). The correlation coefficient indicates how strong the relationship is between the two (Jayalath *et al.*, 2016).

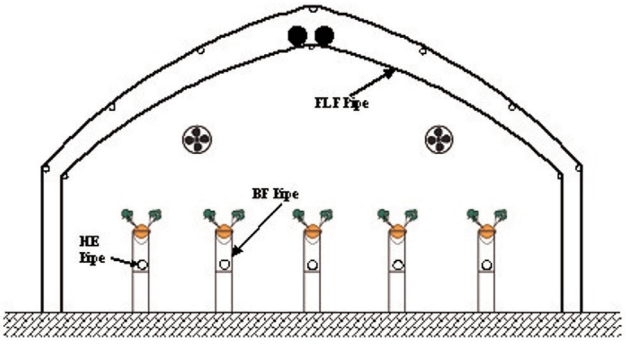

Figure 4. Skeletal view of the RGH showing the pipes in contact with the indoor greenhouse air.

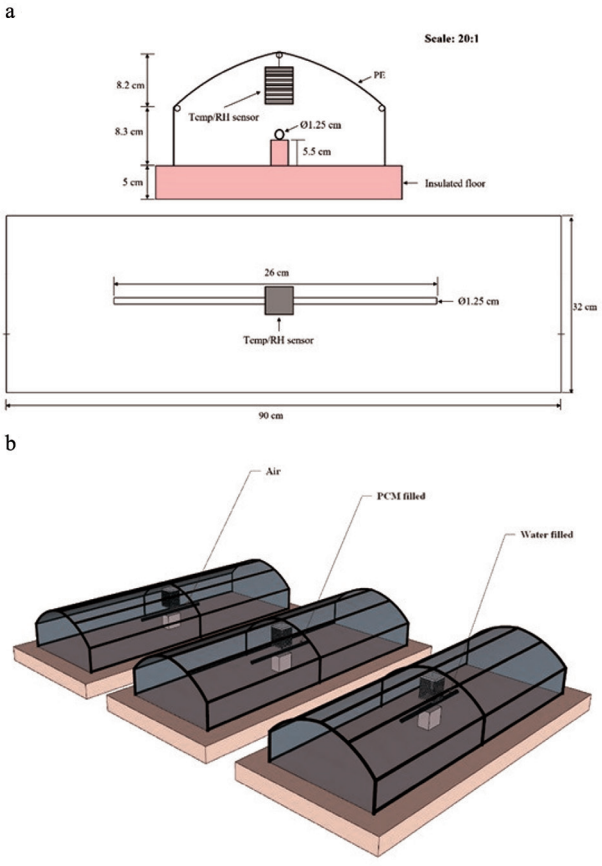

Figure 5 The experimental greenhouse: (**a**) front and plan view of MGs; (**b**) isometric view of MGs.

$$R^2 = 1 - \frac{1}{N}\frac{\sum_{i=1}^{N}(Exp_i - Sim_i)^2}{\sum_{i=1}^{N}(Exp_i - Av)}, Av = \frac{1}{N}\sum_{i=1}^{N} Exp_i \quad \text{(Eq. 7)}$$

$$RMSE = \sqrt{\frac{1}{N}\sum_{i=1}^{N}(Exp_i - Sim_i)^2} \quad \text{(Eq. 8)}$$

$$MAE = \frac{1}{N}\sum_{i=1}^{N}|Exp_i - Sim_i| \quad \text{(Eq. 9)}$$

$$CC = \frac{N\sum Exp_i Sim_i - (\sum Exp_i)(\sum Sim_i)}{\sqrt{N(\sum Exp_i^2) - (\sum Exp_i)^2}\sqrt{N(\sum Sim_i^2) - (\sum Sim_i)^2}} \quad \text{(Eq. 10)}$$

where Av is the mean of the experimental value, Exp_i is the experimental value, Sim_i is the simulated value, and N is the data population.

Results and Discussion

Indoor temperature characteristics

At 90° (E-W) orientation during the winter, the temperature profile of the experimental MGs on day one is shown in Figure 7a. As expected, the three models show similar temperature profiles as energy is gained during the day. Figure 7b shows the experimental difference between the models without the TS on the second night (February 20th) and the models with the TS on the third night (February 21st). The third night temperatures of the MGs were higher due to less energy loss than on the night without the TS. The MG with water as the PCM (water-MG) had generally higher temperatures throughout the night, while the MG without a PCM (air-MG) had the lowest temperatures. In the simulated scenarios (Figure 7c), the variation between the MGs was more pronounced than the variation observed in the experiment; however, the trends were similar. The properties of the PCMs and the TS were used in the simulated scenarios for three days. A comparison of the experimental to the simulated MGs' temperatures is shown in Figure 8. The simulated MGs, which are idealized, show a better response to the ambient temperature. The simulated temperatures are higher than the experimental temperatures on the second day due to the TS-usage scenarios. Figure 8a shows a higher experimental temperature during the third night for the air-MG, which may be attributed to the higher energy received from solar radiation (sunny day), which the sensor shield failed to fully prevent. A similar phenomenon was seen in the other MGs, as shown in Figure 8 b,c. The gap between the experimental and simulated temperatures in the air-MG was the narrowest, while the MG with Vaseline as the PCM (Vaseline-MG) had the widest gap.

Figures 7 and 8 show that the ambient temperature at night was higher than the experimental and simulated MGs temperatures. This may be attributed to a phenomenon called surface temperature inversion (STI). STI is defined by Word Row (2023) as a phenomenon when "air is cooled by contact with a colder surface until it becomes cooler than the overlying atmosphere; this occurs most often on clear nights, when the ground cools off rapidly by long wave radiation …". To confirm this phenomenon, a FLIR thermal imaging camera (model: FLIR-T62101) was used to capture the side view of the water-MG. Figure 9a shows a thermal image of the MG taken at 5 pm, highlighting the stored energy in the pipe. Figure 9 b-d shows that energy dissipation started around 7 pm, thermal equilibrium in the MG began around 11 pm, and the MG temperature fell below the ambient air temperature. A similar experience was reported by Tantau and Akyazi (2017) and Mears and Ph (1998). Compared to the sensor position, the MGs' observed microclimate temperature was lower, which confirms the STI phenomenon. It is worth noting that the height difference between the rooftop and the standard height of measurement for most ambient temperature sensors could have amplified this observation.

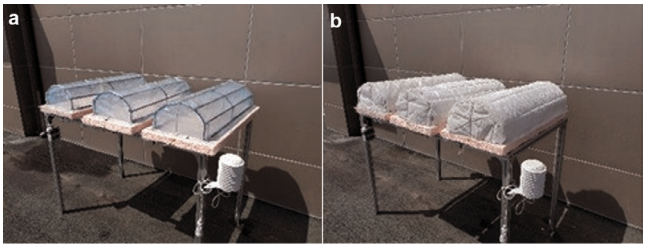

Figure 6. The MG experimental setup, without (**a**) and with (**b**) a thermal screen.

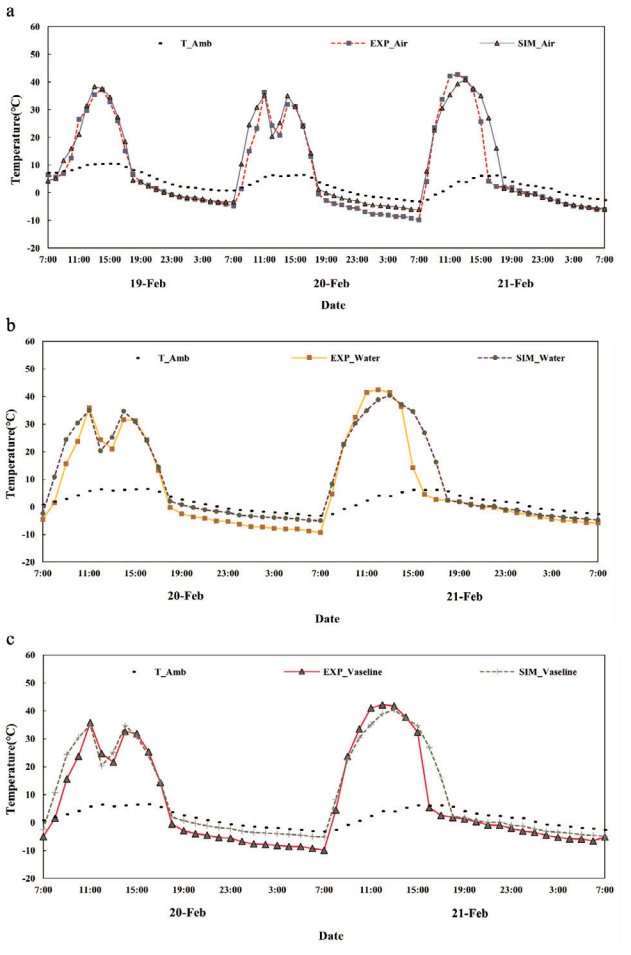

Figure 7 Temperature trends: (**a**) experimental MGs without the PCMs; (**b**) experimental MGs with the PCMs, and (**c**) simulated scenarios.

The simulated results show that the model can predict natural phenomena well, but is not accurate enough to predict further temperature declines in the MGs at the end of the night.

PCM modeling accuracy

This subsection discusses the accuracy of the PCM component in predicting the required energy gain to raise or lower the MGs' air temperature. Figure 10 presents the metrics used to determine the component's accuracy. In Figure 10a, where there were no PCMs, the simulation result matched the experimentation well with an R^2 of 0.96, a CC of 0.98, and errors of 2.8°C (RMSE) and 1.54°C (MAE). The same R^2 and CC values of 0.97 and 0.99, respectively were obtained for both the water- and PCM- MG (Figure 10 b,c). Errors of 2.01°C (RMSE) and 1.33°C (MAE) were obtained for the water-MG and errors of 2.15°C (RMSE) and 1.7°C (MAE) were obtained for the Vaseline-MG. Thus, there was good agreement between the experimental and simulated MGs and a strong relationship between them; in other words, an increase in one causes an increase in the other and *vice versa*. These results conform with earlier research by Jayalath *et al.* (2016) and Cornaro *et al.* (2017), who used the TRNSYS model and IDA ICE, respectively. Therefore, the developed PCM model is suitable for deployment.

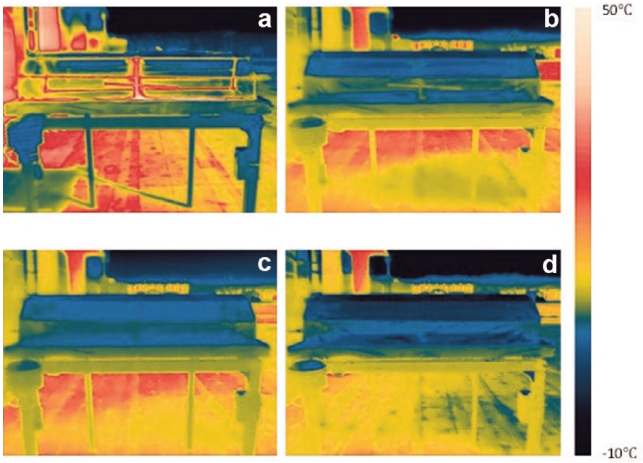

Figure 9 Temperature difference between the water-MG and its environment during: (**a**) late part of the day (5 pm); (**b**) the first (7 pm); (**c**) second (11 pm); and (**d**) third parts of the night (3 am).

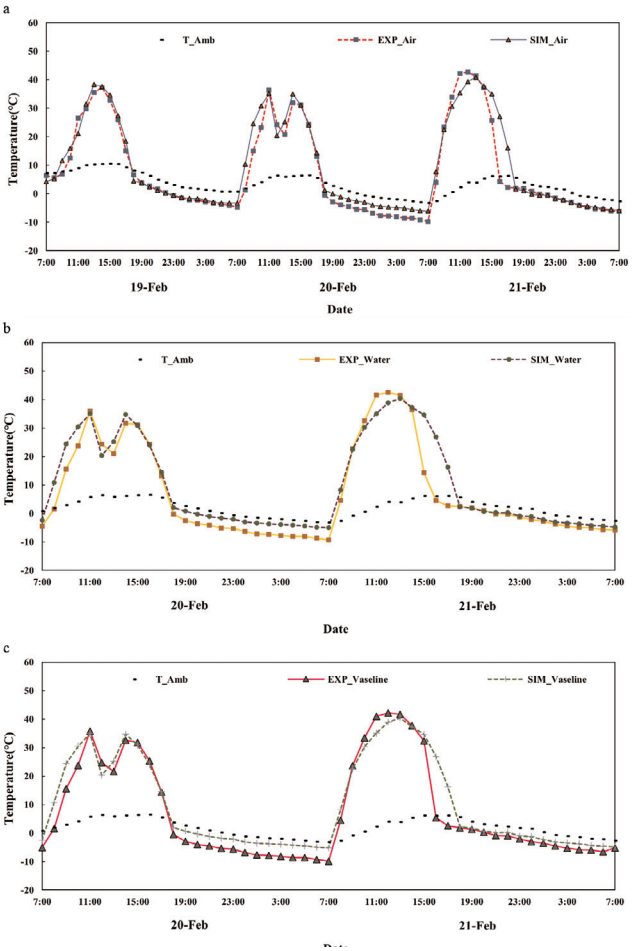

Figure 8. Comparison of the experimental and simulated temperature: (**a**) air vs air; (**b**) water vs water; (**c**) PCM vs PCM.

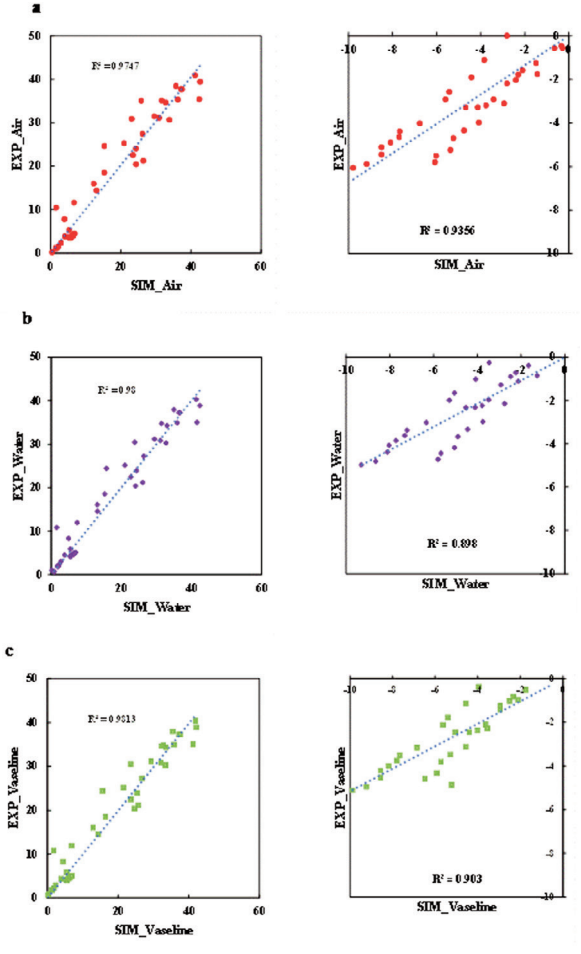

Figure 10. Component validation report: (**a**) air; (**b**) water; (**c**) PCM.

PCM contribution to greenhouse night temperature

This subsection discusses the contribution of the PCM to an actual-size single-layer greenhouse using simulation. In the RGH with a boiler system filled with water, the boiler pipes network's contribution to the stored energy during the day and to the night temperature is also discussed. Figure 11a shows the simulated temperature trend in the actual-size greenhouse. The simulation shows a maximum possible temperature rise of approximately 6.8°C when the ratio of filling-to-greenhouse volume (RFG) was approximately $4.99x10^{-4}$ with water-filled pipes. This result is similar to the experimental research reported by Zhao *et al.* (2023), where water-filled tubes at approximately $4.29x10^{-4}$ RFG caused an average 7°C increase in the night temperature. Thus, it is possible to accurately predict the outcome of the experiment if the PCM model is deployed. The deployment will save construction costs, time, and the associated effective management of an actual-size experimental greenhouse.

Figure 11b presents the contribution of the energy gained by the water in the HE pipes (RFG = $2.75x10^{-4}$ to the night temperature in the RGH. During this experimental period in the RGH, there was no supplemental heating by the boiler, meaning the nighttime temperature (EXP_G) was a product of night gains, excluding the heating system. The contribution was analyzed by simulating the greenhouse temperature with gain (SIM_G) and without gain (SIM_NG) by the water in the HE pipes. The effect could be seen during the day when the temperature was lower because of the cooling effect from the water compared to when the pipes were not filled. There was no significant difference between the two scenarios at night, which could indicate that the energy saved during the day was not enough to raise the nighttime temperature by 1°C.

Unlike in the case when the MGs' internal temperatures were lower than the ambient temperature (see Figure 8), Figure 11a shows that the simulated temperatures were either the same or higher than the ambient temperature (T_Amb). The nighttime release of the energy stored in the soil during the day may be the cause of this phenomenon. During these periods, thermal equilibrium is maintained between the greenhouse microclimate and the ambient air.

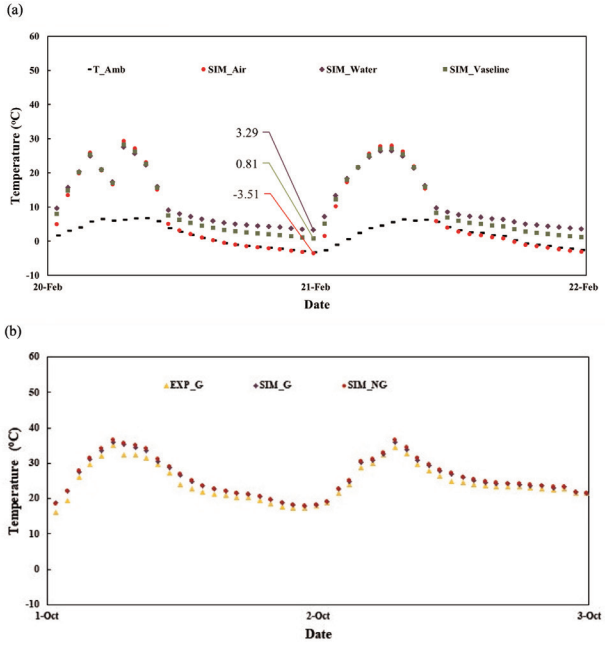

Figure 11. a) Contribution of the PCMs in an actual-size single-layer greenhouse; **b)** reference greenhouse night temperature.

Conclusions

This study set out to address two central research questions: i) whether a phase change material (PCM) component could be developed within TRNSYS 18, and ii) whether such a validated component could be effectively used to evaluate and predict greenhouse thermal behavior.

First, the results clearly demonstrate that a PCM component can indeed be created in TRNSYS 18. A temperature-based PCM component was successfully developed to calculate the energy storage rate arising from the direct interaction between the PCM container and the surrounding air. The component was coupled with greenhouse and weather models and validated experimentally using water as the PCM. The high agreement between simulated and measured temperatures (R^2=0.97, CC=0.99, RMSE=2.01°C, and MAE=1.33 C) confirms that the developed PCM component reliably captures the thermal dynamics of the system. Moreover, the results indicate that water-filled structural elements, such as railing and support pipes, can increase nighttime greenhouse temperatures by up to 7°C, highlighting their strong potential for passive thermal regulation.

Second, the study confirms that once validated, the PCM component can be effectively used to evaluate greenhouse thermal changes. When integrated with other TRNSYS components, the model accurately represents daytime energy charging of the PCM and its subsequent heat release for nighttime heating. This capability enables the assessment of PCM-induced energy gains and losses and supports the evaluation of greenhouse energy demand and internal temperature evolution under varying conditions.

Finally, although the PCM model adopts a simplified formulation, the level of simplification was shown to be acceptable for the primary objective of predicting overall temperature trends. While minor discrepancies were observed between instantaneous simulated and experimental temperatures, these did not compromise the model's ability to reproduce general thermal behavior and energy storage effects.

In summary, this study provides affirmative answers to both research questions: a PCM component can be developed and validated in TRNSYS 18, and it can be reliably used to assess greenhouse thermal performance and energy behavior. The proposed approach offers a practical and computationally efficient tool for analyzing PCM-enhanced greenhouses and similar structures within the TRNSYS simulation environment.

The limitation of this study is the fact that, the effect of hysteresis was not considered in this research, in the future its effect could still be incorporated by rewritting and rebuilding the model equation in TRNSYS Fortran environment.

References

Adesanya MA, Na WH, Rabiu A, Ogunlowo QO, Akpenpuun TD, Rasheed A, et al., 2022. TRNSYS simulation and experimental validation of internal temperature and heating demand in a

glass greenhouse. Sustainability 14:8283.
Akpenpuun TD, Na WH, Ogunlowo QO, Rabiu A, Adesanya MA, et al., 2021a. Effect of glazing configuration as an energy-saving strategy in naturally ventilated greenhouses for strawberry (Seolhyang Sp.) cultivation. J Agric Eng 52:1177.
Akpenpuun TD, Na WH, Ogunlowo QO, Rabiu A, Adesanya MA, et al., 2021b. Effect of greenhouse cladding materials and thermal screen configuration on heating energy and strawberry (Fragaria Ananassa Var. 'Seolhyang') yield in winter. Agronomy 11:2498.
Boussaba L, Lefebvre G, 2021. Investigation of white vaseline as an alternative phase change material for thermal regulation of physiological birth rooms. J Build Eng 44:102669.
Cabeza LF, Castell A, Barrenech C, De Gracia A, Fernández AI, 2011. Materials used as PCM in Thermal energy storage in buildings: a review. Renew Sustain Energy Rev 15:1675-1695.
Chandrasekharan R, Lee ES, Fisher DE, Deokar PS, 2013. An enhanced simulation model for building envelopes with phase change materials. ASHRAE T 119:1-10.
Chanson H, 2009. Turbulent air-water flows in hydraulic structures: dynamic similarity and scale effects. Environ Fluid Mech 9:125-142.
Cornaro C, Pierro M, Adoo Puggioni V, Roncarati D, 2017. Outdoor characterization of phase change materials reach NZEB. Buildings 7:55.
Eydani Asl M, Niezrecki C, Sherwood J, Avitabile P, 2017. Similitude analysis of thin-walled composite I-beams for subcomponent testing of wind turbine blades. Wind Eng 41:297-312.
Jayalath A, Aye L, Mendis P, Ngo T, 2016. Effects of phase change material roof layers on thermal performance of a residential building in Melbourne and Sydney. Energy Build 121:152-158.
Kutty N, Barakat D, Khoukhi M, 2023. A French residential retrofit towards achieving netzero energy target in a Mediterranean climate. Buildings 13:833.
Kuznik F, Virgone J, Johannes K, 2010. Development and validation of a new TRNSYS type for the simulation of external building walls containing PCM. Energy Build 42:1004-1009.
Mazzeo D, Matera N, Cornaro C, Oliveti G, Romagnoni P, De Santoli L, 2020. EnergyPlus, IDA ICE and TRNSYS predictive simulation accuracy for building thermal behaviour evaluation by using an experimental campaign in solar test boxes with and without a PCM module. Energy Build 212:109812.
Mears DR, 1998. Greenhouse glazing effects on heat transfer for winter heating and summer cooling. Available from: https://horteng.envsci.rutgers.edu/workshop/lecture4.pdf
Mu M, Zhang S, Yang S, Wang Y, 2022. Phase change materials applied in agricultural greenhouses. J Energy Storage 49:104100.
Naghibi Z, Carriveau R, Ting DS-K, 2020. Improving clean energy greenhouse heating with solar thermal energy storage and phase change materials. Energy Storage 2:e116.
Najjar A, Hasan A, 2008. Modeling of greenhouse with PCM energy storage. Energy Convers Manag 49:3338-3342.
Nishad S, Krupa I, 2022. Phase change materials for thermal energy storage applications in greenhouses: a review. Sustain Energy Technol Assess 52:102241.
Ogunlowo QO, Akpenpuun TD, Na WH, Rabiu A, Adesanya MA, Addae KS, et al., 2021. Analysis of heat and mass distribution in a single- and multi-span greenhouse microclimate. Agriculture 11:891.
Ogunlowo QO, Akpenpuun TD, Na WH, Adesanya MA, Rabiu A, Dutta P, et al. 2023. Simulation of greenhouse energy and strawberry (Seolhyang Sp.) yield using TRNSYS DVBES: a base case. Solar Energy 266:112196.
Ogunlowo QO, Na WH, Rabiu A, Adesanya MA, Akpenpuun TD, Kim HT, Lee HW, 2022. Effect of envelope characteristics on the accuracy of discretised greenhouse model in TRNSYS. J Agric Eng 53:1420.
Panayiotou GP, Kalogirou SA, Tassou SA, 2016. Evaluation of the application of phase change materials (PCM) on the envelope of a typical dwelling in the Mediterranean region. Renew Energy 97:24-32.
Poulad ME, Fung AS, Naylor D, 2011. Effects of convective heat transfer coefficient on the ability of PCM to reduce building energy demand. Proc. 12th Conf Int Building Performance Simulation Association, Sydney. Available from: https://publications.ibpsa.org/proceedings/bs/2011/papers/bs2011_1202.pdf
Rabiu A, Na WH, Akpenpuun TD, Rasheed A, Adesanya MA, Ogunlowo QO, Kim HT, Lee HW, 2022. Determination of overall heat transfer coefficient for greenhouse energysaving screen using trnsys and hotbox. Biosyst Eng 217:83-101.
Rieradevall J, Montero JI, Llorach-Massana P, Pena J, 2017. Analysis of the technical, environmental and economic potential of phase change materials (PCM) for root zone heating in Mediterranean greenhouses. Renew Energy 103:570-581.
Schranzhofer H, Puschnig P, Heinz A, Streicher W, 2006. Validation of a TRNSYS simulation model for PCM energy storages and PCM wall construction elements. Proc. 10th International Conference on Thermal Energy Storage, Pomona. pp. 2-7.
Seo IW, 2018. Similitude and dimensional analysis. In: Elementary Fluid Mechanics and Lab. Seoul, Seoul National University.
Tantau HJ, Akyazi G, 2017. The low energy greenhouse – Heat Transfer by long wave radiation. Acta Horticulturae 1170:847-854. Tayo OB, 2020. How to calculate accuracy for regression? Accessed: January 12, 2023. Available from: https://pub.towardsai.net/how-do-i-calculate-accuracy-for-regressionec304f3e27b6
TRANSSOLAR Energietechnik. 2017. Multizone building modeling with Type56 and TRNBuild. Available from: https://web.mit.edu/parmstr/Public/Documentation/06-MultizoneBuilding.pdf
Yoo, H. 2024. Average price of water yearly in South Korea from 2012 to 2022. Accessed: May 9, 2025. Available from: https://www.statista.com/statistics/1416838/south-koreaaverage-water-price-yearly/
Zakir E, Ogunlowo QO, Akpenpuun TD, Na WH, Adesanya MA, Rabiu A, et al., 2022. Effect of thermal screen position on greenhouse microclimate and impact on crop growth and yield. Nigerian J Technol Dev 19:417-432.
Zhao M, Liu Y, Bao D, Hu X, Wang N, Liu L, 2023. Study on the influence of solar array tube on thermal environment of greenhouse. Sustainability 15:3127.

Received: 5 August 2025; Accepted: 25 February 2026.

Contributions: Qazeem Opeyemi Ogunlowo, conceptualization, methodology, software, validation, formal analysis, writing - original draft, investigation, visualization. Timothy Denen Akpenpuun, investigation, resources, data curation, writing - review & editing. Wook Ho Na, investigation, resources, data curation, visualization. Misbaudeen Aderemi Adesanya, investigation, writing - review & editing. Anis Rabiu, investigation, writing - review & editing. Adedayo Afeez Azeez, investigation, writing - review & editing. Ayoade Oladele Atere, investigation, writing - review & editing. Hyun-Woo Lee, supervision, resources, funding acquisition. Sangik Lee, resources, writing - review & editing, supervision, project administration, funding acquisition.

Conflict of interest: the authors declare no known competing financial interests or personal relationships that could have appeared to influence the work reported in this paper.

Data availability statement: the source code for the PCM component building and compilation can be found at https://github.com/users/cosmosopy/projects/1. Other data will be available on request.

Funding: this work was supported by the National Research Foundation of Korea(NRF) grant funded by the Korea government (MSIT) (RS-2025-00560277).